Investigation of Some Structural Fusion Materials for (*n*, *α*) Reactions at the 14–15 MeV Energy Region

E. Tel · M. Şahan · A. Aydın · M. Bölükdemir · H. Şahan · F. A. Uğur

Abstract In fusion reactor structures, a serious damage mechanism has been gas production in the metallic resulting from diverse nuclear reactions, mainly through (*n*, *α*) and (*n*, *p*) reactions above a certain threshold energy. The neutron incident energy around 14–15 MeV is enough to excite the nucleus for the reactions such as (*n*, *p*), (*n*, *d*), (*n*, 2*n*), (*n*, *t*), and (*n*, *α*). Design of the fusion reactor, about the 14–15 MeV neutron incident energy reaction cross sections is of great importance for various target nuclei. In this study, the experimental data have been taken only at 14–15 MeV energy regions from EXFOR database. The (*n*, *α*) reactions for some structural fusion materials such as ^{27}Al, ^{51}V, ^{52}Cr, ^{55}Mn, ^{56}Fe and ^{58}Ni have calculated by using evaluated empirical formulas developed by Tel et al. at 14–15 MeV and calculated with the pre-equilibrium models up to 20 MeV. The calculated results are discussed and compared with the experimental data taken from EXFOR database.

Keywords (*n*, *α*) cross-section · Pre-equilibrium reactions · EXFOR file · Empirical formulas

E. Tel (✉) · M. Şahan · H. Şahan · F. A. Uğur
Department of Physics, Faculty of Sciences and Letters,
University of Osmaniye Korkut Ata, Osmaniye, Turkey
e-mail: eyuptel@gazi.edu.tr

A. Aydın
Faculty of Arts and Sciences, Kırıkkale University,
71450 Kirikkale, Turkey

M. Bölükdemir
Department of Physics, Faculty of Arts and Science,
Gazi University, Ankara, Turkey

Introduction

The fast-neutron induced reaction cross-section data have a critical importance on fusion reactors and development for fusion reactor technology [1–4]. In fusion reactor structures, a serious damage mechanism has been gas production in the metallic resulting from diverse nuclear (*n*, *p*) and (*n*, *α*) reactions above a certain threshold energy. The hydrogen isotopes will diffuse out of metallic lattice under high operation temperatures, but the *α* particles will remain in the metal and generate helium gas bubbles [3]. Therefore, the production of helium gas bubbles in the metal crystal lattice will play an important role. Because, it will cause swelling of the structure.

The hybrid reactor is a combination of the fusion and fission processes. The fusion plasma is surrounded with a blanket made of the fertile materials (U^{238} or Th^{232}) to convert them into fissile materials (Pu^{239} or U^{233}) by transmutation through the capture of the high yield fusion neutrons [2–6]. The fertile materials may also undergo a substantial amount of nuclear fission, especially, under the irradiation of the high energetic 14.1 MeV- (D,T) neutrons. So, working out the systematic of the 14–15 MeV neutron reaction cross sections is of great importance for the definition of the excitation function character for the given reaction taking place on various nuclei at energies up to 20 MeV.

For neutron incident energy around 14–15 MeV, a large number of cross sections formulas have been proposed by several authors in the literature [7–11]. Tel et al. [12–18] suggested using the new experimental data to reproduce a new empirical formula of the cross-sections of the (*n*, *p*), (*n*, 2*n*), (*n*, *α*), (*n*, *d*) and (*n*, *t*) reactions. Tel et al. [19] also have investigated the proton incident reaction cross sections and they have obtained new coefficients for the

(p, $n\alpha$) reactions. In the lately work, Hadizadeh and Grimes studied on the calculations of Tel et al. model [20]. And also, Betak et al. [21] investigated the experimental (n, p) cross sections of ^{112,115,117}Sn isotopes by using Tel et al. and other researches' formulas . Goyal and Kishore [22] have been studied the empirical formulae with two parameters for the evaluation of (n,α) reaction cross-sections . In this study, neutron incident reaction cross sections for some for some structural fusion materials such as ^{27}Al(n, α)^{24}Na, ^{51}V(n, α)^{48}Sc, ^{52}Cr (n, α) ^{49}Ti, ^{55}Mn(n, α)^{52}V, ^{56}Fe (n, α) ^{53}Cr, and ^{58}Ni(n, α) ^{55}Fe have been calculated up to 20 MeV by using the equilibrium and pre-equilibrium models. In these calculations, the pre-equilibrium calculations involve the new evaluated the geometry dependent hybrid model, hybrid model and full exciton model [23, 24]. The reaction equilibrium component was calculated with a traditional compound nucleus model developed by Weisskopf and Ewing [25]. Additionally in the present work, the (n, α) reaction cross-sections have calculated by using evaluated empirical formulas developed by Tel et al. at 14–15 MeV energy. The calculated results are discussed and compared with the experimental data taken from EXFOR database [26].

Theoretical Calculations Methods of Nuclear Reaction Cross Sections

The nuclear reaction models are frequently needed to provide the estimation of the particle–induced reaction cross-sections, especially if the experimental data are not obtained or on which they are hopeless to measure the cross-sections due to the experimental difficulty. The nuclear reaction model calculations performed includes the direct-interaction, pre-equilibrium, and equilibrium (compound) nucleus contributions. The direct-interaction reactions occur on a very short time scale (about $\leq 10^{-22}$ s). The compound (equilibrium) nucleus reactions however occur on a very much longer time scale ($\cong 10^{-16}$ to 10^{-18} s). Pre-equilibrium processes play an important role in nuclear reactions induced by light projectiles with incident energies above about 8–10 MeV. The pre-equilibrium reactions occur on time scale about $\cong 10^{-18}$ to 10^{-20} s (between direct and equilibrium reaction time scale). The pre-equilibrium and equilibrium emission spectrum are given in the full exciton model [24],

$$\frac{d\sigma_{ab}}{d\varepsilon_b}(\varepsilon_b) = \sigma_{ab}^r(E_{inc})D_{ab}(E_{inc})\sum_n W_b(E,n,\varepsilon_b)\tau(n), \qquad (1)$$

where $D_{ab}(E_{inc})$ is a coefficient which takes into account the decrease in the available cross-section due to the particle emission by direct interactions with low excitation

energy levels of the target nucleus. $\sigma_{ab}^r(E_{inc})$ is the cross-section of the reaction (a, b), W_b (E,n,ε_b) is the probability of the emission of a particle type b with energy ε_b from a state with n excitons and excitation energy E of the compound nucleus, $\tau(n)$ is the solution of the master equation which represents the time during which the system remains in a state of n excitons.

The intra nuclear cascade calculations results indicated that the exciton model gives only a prescription for calculating the shape of the pre-equilibrium spectrum and the exciton model deficiency resulted from a failure to properly reproduce enhanced emission from the nuclear surface. In order to provide a first order correction for this deficiency the hybrid model was reformulated by Blann [27, 28]. The hybrid model has been developed by Blann and Vonach considered as density distribution of nuclei as geometry dependent hybrid model (GDH) [29]. In the density dependent version, the GDH model takes into account the density distribution of the nucleus [29]. This means a longer mean free path at the surface of the nucleus because of a lower density, and a limit to the depth of the holes below the Fermi energy. The differential emission spectrum is given in the GDH as

$$\frac{d\sigma_v(\varepsilon)}{d\varepsilon} = \pi\hat{\lambda}^2 \sum_{\ell=0}^{\infty} (2\ell+1)T_\ell P_v(\ell,\varepsilon) \qquad (2)$$

where $\hat{\lambda}$ is the reduced de Broglie wavelength of the projectile and T_1 represents the transmission coefficient for the lth partial wave. $P_v(\ell,\varepsilon)$ is number of particles of the type v (neutrons and protons) emitted into the unbound continuum with channel energy between ε and $\varepsilon + d\varepsilon$ for the lth partial wave. The GDH model is made according to incoming orbital angular momentum l in order to account for the effects of the nuclear-density distribution.

Empirical Neutron Induced Reaction Cross-Section Formulas at 14–15 MeV

The empirical cross-sections of reactions induced by fast neutrons can be approximately expressed as follows:

$$\sigma(n,x) = C\sigma_{ne} \exp[as] \qquad (3)$$

where σ_{ne} is the neutron non-elastic cross-section, and the C and a coefficients are the fitting parameters determined from least-squares method for different reactions. The non-elastic cross-sections have been measured intensely for many nuclides in the MeV range, enabling us to find out their variation with atomic mass. The neutron non-elastic cross-section is given by πR^2, where R is the nuclear radius and

$$\sigma_{ne} = \pi r_0^2 (A^{1/3} + 1)^2, \qquad (4)$$

where, $r_0 = 1.2 \times 10^{-13}$ cm and A is the mass number of target nuclei. Equation 3 represents the product of two factors, the each of which might be assigned to a stage of nuclear reaction within the framework of the statistical model of nuclear reactions. The exponential term represents the escape of the reaction products from a compound nucleus. It has a strong $s = (N−Z)/A$ dependence implied by Eq. 3, where N and Z are the neutron and proton number of target nuclei, respectively.

Tel et al. [12–18] suggested using the new experimental data to reproduce a new empirical formula of the cross-sections of the (n, p), $(n, 2n)$, (n, α), (n, d) and (n, t) reactions at 14–15 MeV neutron incident energy . The Tel et al. [14] (n, α) formulas for $20 \leq A \leq 239$ target nuclei have been given as follows (in mb) at $E_n = 14–15$ MeV

$$\sigma(n, \alpha) =$$
$$\begin{cases} 14.43(A^{1/3}+1)^2 \exp[-32.17s] & \text{for Even - Z, Even - N} \\ 19.41(A^{1/3}+1)^2 \exp[-35.97s] & \text{for Even - Z, Odd - N} \\ 17.93(A^{1/3}+1)^2 \exp[-34.04s] & \text{for Odd - Z, Even - N} \end{cases}$$
$$(5)$$

Results and Discussion

The nuclear model software has become indispensible in modern nuclear data evaluation. The adjustable parameters of the nuclear model code should be fitted to reproduce the experimental data available for the nucleus under study. In this study, the theoretical calculations have been made in the framework of the full exciton model using PCROSS computer code [24]. The full exciton model calculations includes the equilibrium and pre-equilibrium nucleus contributions in Eq. 1. We used the standard Weisskopf–Ewing theory for equilibrium calculations. The term equilibrium (compound) reaction is commonly used for two different processes: (1) capture of projectile in the target nucleus to form o compound nucleus, (2) multiple emission from the chain of excited residual nuclides following the binary reaction. Equilibrium emission is calculated according to Weisskopf–Ewing model [25] by neglecting the angular momentum. In the equilibrium model, the basic parameters are binding energies, inverse reaction cross-section, the pairing energy and the level-density parameters. In the full exciton model calculations, we used the initial exciton number as $n_o = 1$ of 1 neutron and 0 hole: single particle level density parameter g is equal to $A/13$ in the exciton model calculation, where A is the mass number. Level density expression given by Dilg [30] was used in the evaporation model calculation. Particle-hole state density expression reported by Williams was used in the pre-equilibrium model calculations [31]. The reaction cross-sections and the inverse cross-sections were obtained using the optical potential parameters by Wilmore et al. [32], Bechetti et al. [33], Huizenga et al. [34] for neutrons, protons and alpha particles, respectively. The octupolar and quadrupolar oscillations are only considered. The ω_2, β_2, values for even nuclei have been taken from [35]. In the case of odd nuclei, on the assumption of a weak bond, the values corresponding to the neighboring even nucleus are used. The ω_3 value has been taken from [36]. The octupolar deformation parameters have been calculated from

$$\beta_3^2 = (2\lambda + 1)\omega_3[\text{MeV}]/1,000 \qquad (6)$$

The calculated results are compared with the experimental data in Figs. 1, 2, 3, 4, 5, 6. The experimental taken from EXFOR database [26]. In this study, ALICE/ASH code
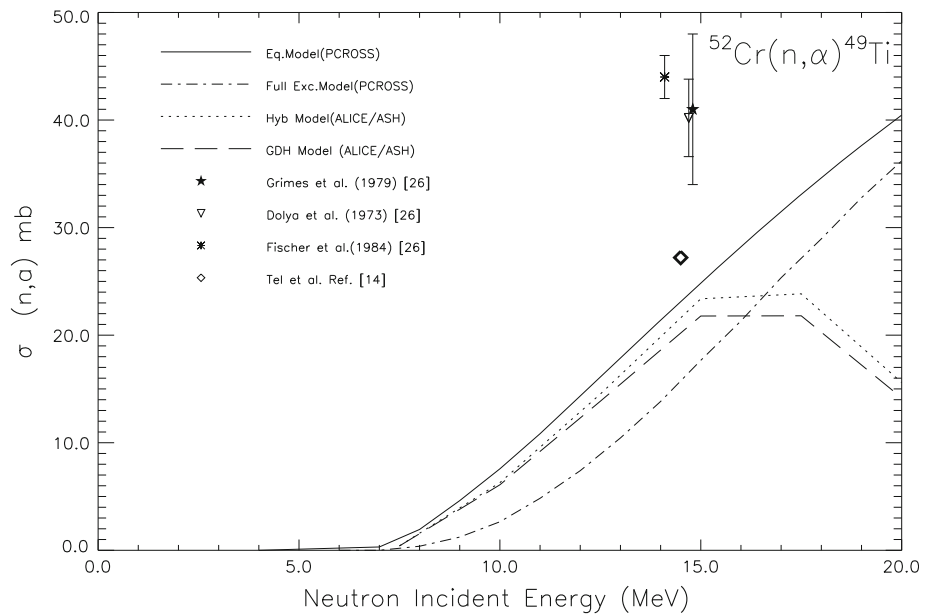

Fig. 1 The comparison of calculated excitation function of $^{27}\text{Al}(n, \alpha)$ ^{24}Na reaction with the values reported in [26]
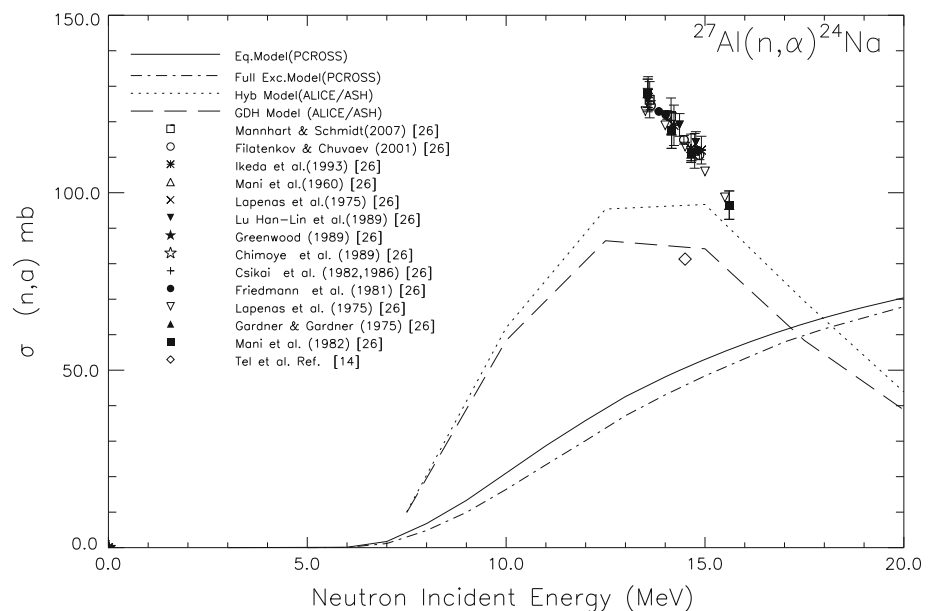
Fig. 2 The comparison of calculated excitation function of $^{51}V(n,\alpha)\,^{48}Sc$ reaction with the values reported in [26]
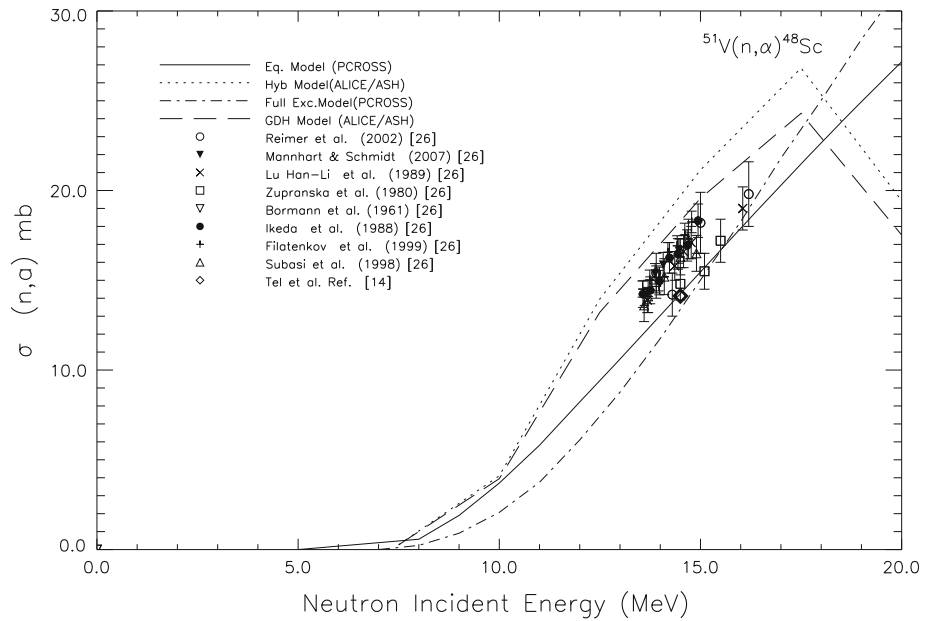
Fig. 3 The comparison of calculated excitation function of $^{52}Cr(n,\alpha)\,^{49}Ti$ reaction with the values reported in [26]

was used in the calculations of the hybrid and GDH model [23]. The ALICE/ASH code is an advanced and modified version of the ALICE codes. The ALICE/ASH code can be applied for the calculation of excitation functions, energy and angular distribution of secondary particles in nuclear reactions induced by nucleons and nuclei with the energy up to 300 MeV. The initial exciton number as $n_o = 3$ and the exciton numbers (for protons and neutrons) in the calculations for neutron induced reactions as

$$_3X_n = 2\frac{(\sigma_{np}/\sigma_{nn})Z + 2N}{2(\sigma_{np}/\sigma_{nn})Z + 2N},\, _3X_p = 2 - _3X_n, \quad (7)$$

where σ_{xy} is the nucleon–nucleon interaction cross-section in the nucleus. The ratio of nucleon–nucleon cross-sections

calculated taking into account to Pauli principle and the nucleon motion is parameterized

$$\sigma_{pn}/\sigma_{pp} = \sigma_{np}/\sigma_{nn}$$
$$= 1.375 \times 10^{-5}T^2 - 8.734 \times 10^{-3}T + 2.776$$

$$(8)$$

where T is the kinetic energy of the projectile outside the nucleus. In details, the other all code model parameters can be found in [23].

In this study, (n,α) reaction cross-sections for some structural fusion materials such as ^{27}Al, ^{51}V, ^{52}Cr, ^{55}Mn, ^{56}Fe, and ^{58}Ni have been calculated with the equilibrium and pre-equilibrium reaction models at 14–15 MeV energy are given in Table 1 and results are given in

Fig. 4 The comparison of calculated excitation function of ^{55}Mn(n, α) ^{52}V reaction with the values reported in [26]
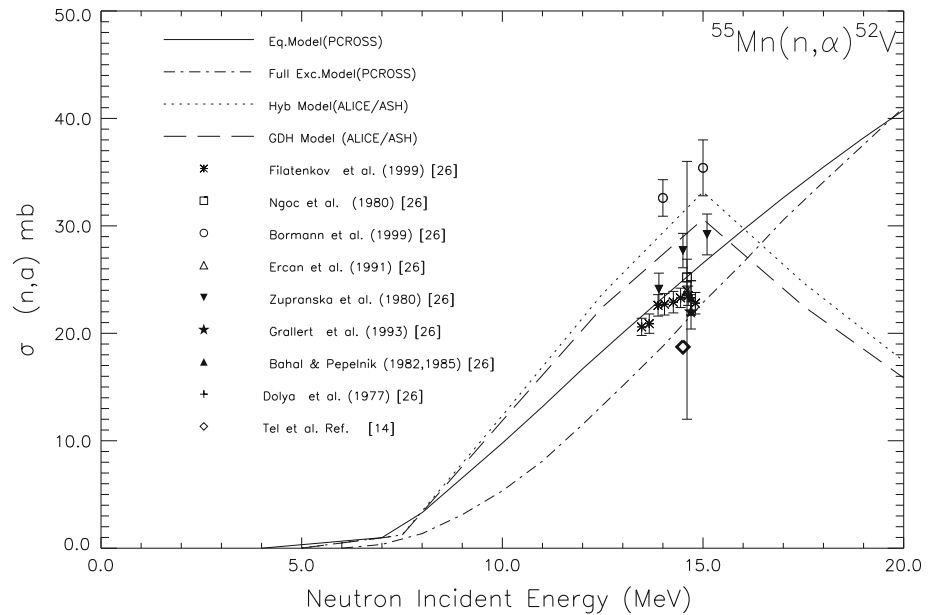
Fig. 5 The comparison of calculated excitation function of ^{56}Fe(n, α) ^{53}Cr reaction with the values reported in [26]
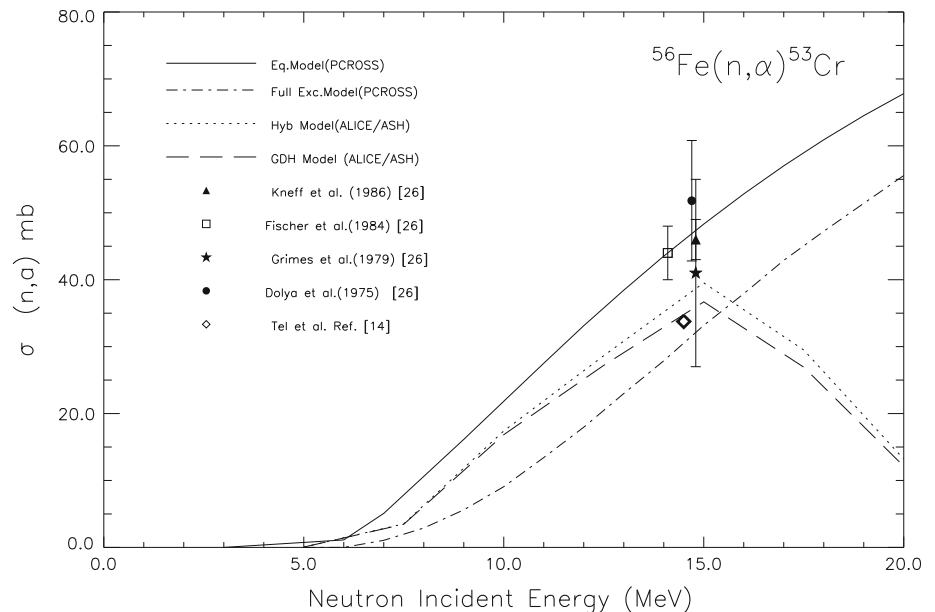

Figs. 1, 2, 3, 4, 5, 6 as a function of incident neutron energy.

In Table 1, first column shows the names of nuclei according to the target mass number. Equilibrium and full exciton model calculations (with PCROSS) for 5–20 MeV energy [24] are listed in the next two columns, respectively. Hybrid and GDH model calculations (with ALICE/ASH) [23] are given in the fourth and fifth columns, respectively. Similarly, the data obtained with hybrid and GDH model were given for 5–20 MeV energy. Data from the empirical formula developed by Tel et al. [14] are given in the sixth column. The some experimental data taken from EXFOR [26] between 14 and 15 MeV are given in final column. As mentioned in previous paragraph, the

calculated results are compared with the experimental data in Figs. 1, 2, 3, 4, 5, 6. The experimental taken from EXFOR [26] are shown with different symbols in Figs. 1, 2, 3, 4, 5, 6. The cross-section obtained from empirical formula developed by Tel et al. [14] at 14–15 MeV energy is also given with equilateral quadrangle in these all figures.

The comparison of the calculated cross-section of ^{27}Al(n, α)^{24}Na reaction up to 5–20 MeV is given in Fig. 1. As seen from the Fig. 1, the experimental data were obtained thirteen different authors from EXFOR [26]. All experimental data for ^{27}Al(n, α)^{24}Na are higher than four theoretical models. The hybrid model is harmonious with some experimental data (for example Mani et al. and Lapenas et al. [26]) at ≈15.5 MeV energy. From the

Fig. 6 The comparison of calculated excitation function of ^{58}Ni(n, α) ^{55}Fe reaction with the values reported in [26]
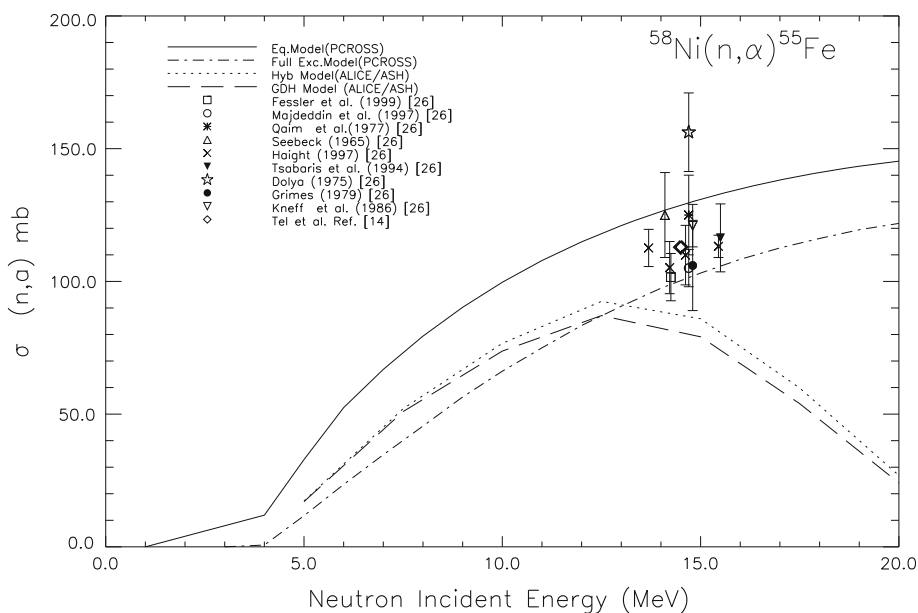
empirical formula developed by Tel et al. [14] cross-section value is 81.31 mb at 14–15 MeV and this cross-section is almost consistent with GDH model at this energy interval.

The comparisons of the calculated cross-sections of ^{51}V(n, α)^{48}Sc reaction up to 20 MeV is given in Fig. 2. The experimental data from EXFOR [26] were obtained from eight different researches. The experimental energy values between 13.57 MeV and 16.20 MeV have the cross-section changing from 14.23 mb (Ikeda et al. 1988) to 19.80 mb (Remier et al. 2002), respectively. All four model calculations at energy region up to 14–15 MeV are in good agreement with the experimental data for alpha induced reactions in this study. The cross-section from the empirical formula developed by Tel et al. [14] is determined to be 14.12 mb at 14–15 MeV and this cross-section is almost consistent with both experimental data and theoretical models (especially, Equilibrium model calculations).

Figure 3 shows comparisons of the calculated cross-sections of ^{52}Cr(n, α)^{49}Ti reactions up to 5–20 MeV. We were able to find only three experimental data from different researches from EXFOR [26]. From these data, we see that their cross-section values are higher than all four theoretical models. From Table 1, these cross-sections are 41.00 mb by Grimes et al. (1979), 40.20 mb by Dolya et al. (1973), and 44.00 mb by Fischer et al. [26] (detail information can be found at). The cross-section from the empirical formula developed by Tel et al. [14] was found to be 27.21 mb at 14–15 MeV energy. This cross-section was found lower than all experimental data but is close to the theoretical models, especially with Equilibrium model calculations.

Figure 4 shows the calculated cross sections of ^{55}Mn(n, α)^{52}V reactions up to 5–20 MeV. From EXFOR [26], experimental data from eight different researches were obtained. As seen from Fig. 4, the experimental data for neutron induced reactions are in close agreement with all four model calculations at energy region up to 14–15 MeV in this study. Especially, data from Filatenkov et al. [26] lie between full exciton and equilibrium Models (PCROSS). Moreover, data by Zupranska et al. [26] increases with increasing energy between full exciton and equilibrium Models and consistents with GDH model. It was found the cross-section to be 18.73 mb at 14–15 MeV energy from the empirical formula developed by Tel et al. [14] and is in good agreement with the experimental data and theoretical models, especially full exciton and equilibrium Model.

The calculated cross-sections of ^{56}Fe(n,α)^{53}Cr reactions up to 5–20 MeV is shown in Fig. 5. As seen from Fig. 5, experimental data have been obtained from four different researches using EXFOR [26]. The experimental data are also agreement all four model calculations (especially equilibrium model). As seen from Table 1, the cross-section data for ^{56}Fe(n,α)^{53}Cr from Tel et al. [14] was calculated to be 33.76 mb at 14–15 MeV from Tel et al. [14]. This is consistent with the calculation of GDH model (with ALICE/ASH) at same energy interval.

Figure 6 shows the calculated cross-sections of ^{58}Ni(n, α)^{55}Fe reactions between 5 and 20 MeV. The experimental data were obtained from nine different researches using EXFOR [26]. The experimental cross-section data change from 101.60 mb (Fessler et al. (1999) [26]) to 156.20 mb (Dolya (1975) [26]) between 14.50 and 14.70 MeV energy, respectively. The all experimental data are lying between

Table 1 Experimental and theoretical (n, α) cross-sections (in mb) at 14–15 MeV. The experimental data taken from [26]

	Equ. model	Full ext. model	Hyb. model	GDH model	Tel et al.	Exp. results
^{27}Al(n,α)	53.03	48.39	96.69	84.20	81.31	111.80
						110.60
						112.00
						114.20
						111.00
						113.90
^{51}V(n, α)	15.47	15.01	21.14	19.56	14.12	16.63
						14.20
						16.56
						17.30
						14.80
						15.80
^{52}Cr(n, α)	24.83	17.65	23.38	21.77	27.21	36.00
						40.20
						44.00
^{55}Mn (n, α)	26.53	22.86	33.16	30.62	18.73	23.50
						24.00
						25.20
						27.70
						22.00
						23.30
^{56}Fe (n, α)	48.30	33.17	39.53	36.68	33.76	46.00
						51.80
						44.00
						41.00
^{58}Ni (n, α)	130.90	103.12	85.92	79.11	112.90	101.60
						105.00
						125.00
						109.90
						106.00
						121.00

full exciton and equilibrium Model calculations. The cross-section from Tel et al. [14] empirical formula is 112.90 mb at 14–15 MeV and is almost consistent with all experimental data all model calculations.

Consequently, the empirical formulas use the equilibrium model and ignore an important role of the pre–equilibrium mechanism of particle emission. The pre–equilibrium calculations are in better agreement with the experimental data than the empirical formulas. Because, the pre–equilibrium systematic are based on the use of analytical expressions for calculation of particle emission. The empirical formulas given in Eq. 5, for the (n, α) reaction can be considered to provide a very useful tool for estimating quickly, in view of the poor agreement with experiment sometimes provided by calculations based on the semi-empirical systematic. This study helps to show the way to the future experimental studies.

Summary and Conclusions

In this study, (n, α) reactions for some structural fusion materials have been investigated up to 20 MeV incident neutron energy. The calculated results have been also compared with the available experimental values in literature. The results can be summarized and concluded as follows:

1. The experimental cross-section values for ^{52}Cr$(n, \alpha)^{49}$Ti obtained from EXFOR reactions are higher than all theoretical calculation models.
2. The calculated and experimental cross-sections are the lowest for ^{51}V$(n, \alpha)^{48}$Sc reactions for the considered nuclei in this study.
3. Except from ^{52}Cr nucleus, the calculated pre-equilibrium and empirical reaction cross-sections formula

show the agreement with experimental data for the considered nuclei.

4. The empirical cross-section formula developed by Tel et al. is almost consistent with pre-equilibrium and equilibrium model at 14–15 energy interval considered nuclei in this study

The empirical formulas for the (n, α) reaction can be considered to provide a very useful tool for estimating quickly at 14–15 energy interval.

References

1. M. Walt, in *Fast Neutron Physics, Part I: Techniques*, ed. by J. B. Marion and J. L. Fowler, (Interscience, New York, 1960), p. 509
2. S. Şahin, M. Übeyli, J. Fusion Energ. **27**, 271 (2008)
3. S. Şahin, M. Übeyli, Energy. Conver. Manage. **45**, 1497 (2004)
4. S. Şahin, T. Al-Kusayer, M.A. Raoof, Fusion. Technology **10**, 84 (1986)
5. S. Şahin, H.M. Şahin, K. Yıldız, Annals. Nucl. Energy. **29**, 1641 (2002)
6. S. Şahin, H.M. Şahin, K. Yıldız, A. Acır, Kerntechnik **70**, 4 (2005)
7. R.A. Forrest, J. Kopecky, Nucl. Eng. Des. Fusion. **82**, 73 (2007)
8. M. Belgaid, M. Asghar, Appl. Radiat. Isot. **49**, 1497 (1998)
9. Yu.A. Korovin, Yu.A. Konobeyev, Nucl. Instr. Meth. **B.103**, 15 (1995)
10. E. Tel, Ş. Okuducu, A. Aydin, B. Şarer, G. Tanir, Acta. Phys. Slov. **54**(2), 191 (2004)
11. S.L. Goyal, P. Gur, Pramana **72**(2), 355 (2009)
12. E. Tel, B. Şarer, Ş. Okuducu, A. Aydin, G. Tanir, J. Phys. G. Nucl. Part. Phys. **29**, 2169 (2003)
13. E. Tel, A. Aydin, G. Tanir, Phys. Rev. C **75**, 034614 (2007)
14. E. Tel, Ş. Okuducu, M.H. Bölükdemir, G. Tanir, Int. J. Mod. Phys. E. **17**(3), 567 (2008)
15. E. Tel, A. Aydin, A. Kaplan, B. Şarer, J. Fusion Energ. **27**(3), 188 (2008)
16. A. Aydin, E. Tel, A. Kaplan, J. Fusion Energ. **27**(4), 308 (2008)
17. A. Aydin, E. Tel, A. Kaplan, B. Şarer, J. Fusion Energ. **27**(4), 314 (2008)
18. M.H. Bölükdemir, E. Tel, N.N. Aktı, J. Fusion Energ. **29**, 13 (2010)
19. E. Tel, E.G. Aydin, A. Aydin, A. Kaplan, Appl. Radiat. Isot. **67**(2), 272 (2009)
20. M.H. Hadizadeh, S.M. Grimes, Nucl. Sci. Eng. **160**(2), 207 (2008)
21. E. Betak, R. Mikolajczak, J. Staniszewska, S. Mikolajewski, E. Rurarz, Radiochim. Acta **93**, 311 (2005)
22. S.L. Goyal, N. Kishore, Indian. J. Phys. **84**(5), 553 (2010)
23. C.H.M. Broeders, A.Yu. Konobeyev, Yu.A. Korovin, V.P. Lunev, and M. Blann, FZK 7183 (2006) http://bibliothek.fzk.de/zb/berichte/FZKA7183.pdf
24. R. Capote, V. Osorio, R. Lopez, E. Herrera, M. Piris, Final report on research contract 5472/RB, INDC(CUB)-004 (Higher Institute of Nuclear Science and Technology, Cuba), Translated by the IAEA on March 1991 (PCROSS program code)
25. V.F. Weisskopf, D.H. Ewing, Phys. Rev. **57**, 472 (1940)
26. EXFOR/CSISRS (Experimental Nuclear Reaction Data File), Brookhaven National Laboratory, National Nuclear Data Center, (http://www.nndc.bnl.gov/exfor/) (2009)
27. M. Blann, Phys. Rev. Lett. **27**, 337 (1971)
28. M. Blann, Annu. Rev. Nucl. Sci. **25**, 123 (1975)
29. M. Blann, H.K. Vonach, Phys. Rev. C **28**, 1475 (1983)
30. W. Dilg, W. Schantl, Vonach, H.M. Uhl, Nucl. Phys. **A217**, 269 (1973)
31. F.C. Williams, Nucl. Phys. A. **166**, 231 (1971)
32. D. Wilmore, P.E. Hodgson, Nucl. Phys. **55**, 673 (1964)
33. F.D. Becchetti, G.W. Greenlees, Phys. Rev. **182**, 1190 (1969)
34. J.R. Huizenga, G. Igo, Nucl. Phys. **29**, 462 (1962)
35. S. Raman et al., Data Nucl. DataTables. **36**, 1 (1987)
36. C.M. Lederer, V.S. Shirley (eds.), *Table of Isotopes*, 7th edn. (Wiley, London, 1978)